NANO LETTERS

2008
Vol. 8, No. 8
2419-2422

# Ordered Arrays of ZnO Nanorods Grown on Periodically Polarity-Inverted Surfaces

**Sang Hyun Lee,*,† Tsutomu Minegishi,‡ Jin Sub Park,‡ Seung Hwan Park,‡ Jun-Seok Ha,† Hyo-Jong Lee,† Hyun-Jae Lee,† Sungmo Ahn,§ Jaehoon Kim,§ Heonsu Jeon,§ and Takafumi Yao†,‡**

*Center for Interdisciplinary Research, Tohoku University, Aramaki, Aoba-ku, Sendai 980-8578, Japan, Institute for Materials Research, Tohoku University, Sendai 980-8577, Japan, and Department of Physics and Astronomy, Inter-University Semiconductor Research Center, Seoul National University, Seoul 151-747, Korea*

*Received May 10, 2008; Revised Manuscript Received June 4, 2008*

## ABSTRACT

**Periodically polarity inverted (PPI) ZnO templates were fabricated using molecular beam epitaxy by employing MgO buffer layers. The polarity of ZnO film was controlled by the transformation of crystal structure from hexagonal to rocksalt due to the thickness of the MgO buffer layers. The polarity of ZnO in the PPI template was confirmed by AFM and PRM measurement. Higher growth rate and lower current value under positive supplied voltage in the region of Zn-polar were measured with comparing to that of O-polar. Holographic lithographic technique was employed for the realization of submicron pattern of periodical inverted polar ZnO over large area. After reaction using a carbothermal reduction, spatially well-separated ZnO nanorods with pitch of submicron were only observed in the Zn-polar regions. The possible reason for the difference of surface characteristics was considered as being due to the configuration of dangling bonds according to polarity.**

The study on the control of quasi one-dimensional (1D) nanostructures is an important step toward deeper understanding of material characteristics as well as their potential applications to electronic, optoelectronic, electrochemical, and electromechanical devices.[1–3] Significant advance has been made in the control of size and morphology of 1D nanostructures fabricated by vapor−solid−liquid (VLS) growth via lithographic techniques using photon beam, electron beam, nanosphere, anodic aluminum oxide, and nanoimprint.[4]

Here we report on the fabrication of ordered arrays of ZnO nanorods using controlled polar surfaces of ZnO templates. Polar surfaces are generally produced by accumulating normal dipole moment in ionic crystals which consist of alternating layers of oppositely charged ions stacked perpendicular to the polar surfaces. ZnO crystallizes in hexagonal wurtzite-type structure, which consists of alternating planes of four-fold coordinated $O^{2-}$ and $Zn^{2-}$ ions along the <0001> crystallographic direction. These two polar surfaces which are positively charged (0001)-Zn and negatively charged $(000\bar{1})$-O planes have different chemical and physical properties. ZnO nanostructures are widely used in catalyst, gas sensing, laser and microelectronic devices. [5–7] The morphology of ZnO nanostructures is dependent on growth condition and surface energy. The geometric, electronic, and defect characteristics of the surface of nanostructures play an important role in all of applications.

Experimental studies on the growth behaviors on different polar surface of ZnO have been recently carried out. The formation of nanocantilever arrays on chemically active Zn polar surface of ZnO ribbons was reported by Wang and co-workers.[8] It was reported that ZnO nanowires can be grown only on Zn-polar surfaces, while 2D growth favors O-polar surfaces.[9] In the case of layer growth on nonpolar c-sapphire substrates, it is reported that O-polar layers grow directly on c-sapphire, while Zn-polar ZnO layers grow either on MgO buffer thicker than 3 nm or on CrN buffer predeposited on c-sapphire. [10–12] In this paper, we demonstrate the fabrication of well-ordered array of 1D ZnO nanorods with the growth sites being controlled by exploiting the polarity dependent surface nature of ZnO.

Figure 1 shows a schematic of the fabrication process of ordered ZnO nanorod arrays on periodically polarity inverted (PPI) templates: C-plane sapphire substrates were first cleaned in acetone, then methanol for 10 min, followed by

* Corresponding author. Tel: +81-22-795-7281. Fax: +81-22-795-6167. E-mail: shlee7579@gmail.com.
† Center for Interdisciplinary Research, Tohoku University.
‡ Institute for Materials Research, Tohoku University.
§ Seoul National University.

10.1021/nl801344s CCC: $40.75 
**Published on Web 06/25/2008**

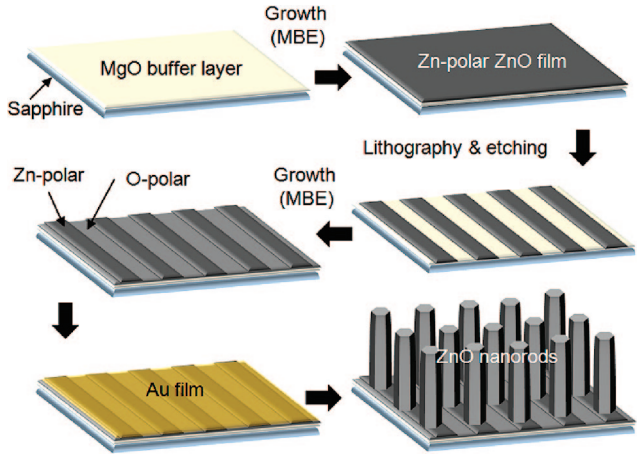


**Figure 1.** Schematic diagram of periodic polar inverted ZnO templates for ordered ZnO nanorod arrays.

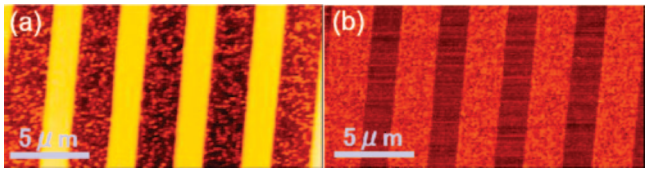


**Figure 2.** (a) AFM and (b) PRM image of the surface of the PPI template.

acid treatment in piranha ($H_2SO_4/H_2O_2$ = 3:1) for 5 min at 160 °C. After rinsing in deionized water, the substrates were mounted in a molecular beam epitaxy (MBE) chamber. The polarity of ZnO layers grown on c-plane sapphire can be controlled by tuning the thickness of the MgO buffer. Typically, the critical thickness of MgO buffer for transformation of the polarity of ZnO film is 2.7 nm: O-polar ZnO film is formed on MgO buffer with the thickness below 2.7 nm, while Zn-polar ZnO for a on MgO buffer thicker than 2.7 nm.[12]

At first Zn-polar ZnO film was grown on thick MgO buffer with typical thickness of 8 nm. Then 1D periodic patterning was performed using chemical/dry etching process via photo- or holographic lithography,[13] in which parts of ZnO layers were etched away and the thickness of the MgO buffer was partially etched down to below 2.7 nm. The consecutive growth of ZnO allowed the formation of O-polar ZnO on the thin MgO, while the growth of Zn-polar ZnO continued on the unetched Zn-polar ZnO layers.

Figure 2a,b displays the atomic force microscopy (AFM) and piezoelectric-response microscopy (PRM) images of a PPI ZnO template. A clear periodically stripped pattern is observed with the widths of line and stripe being 2 $\mu$m each. The Zn-polar regions (bright) are thicker than the O-polar regions (dark) due to higher growth rate on Zn-polar ZnO.[10] In the PRM measurement, the conductive cantilever is grounded and an AC voltage is applied to the sample while scanning the sample surface. The bright regions in Figure 2b are negative domains with negative surface polarization charges, while the darker regions are positive domains with positive surface polarization charges. We confirm that the thick and the thin regions correspond to Zn- and O-polar ZnO, respectively.

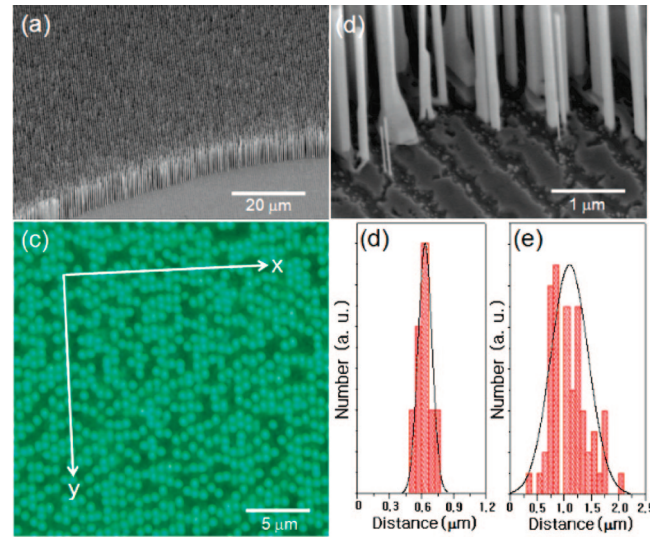


**Figure 3.** (a) Low-magnification and (b) enlarged SEM images of ZnO nanorods grown on the PPI ZnO template. (c) Optical microscope top-view image of the ZnO nanorods under UV illumination. The plots of (d) and (e) show the distance distribution of adjacent ZnO nanorods with (*x*-axis) or without (*y*-axis) patterning.

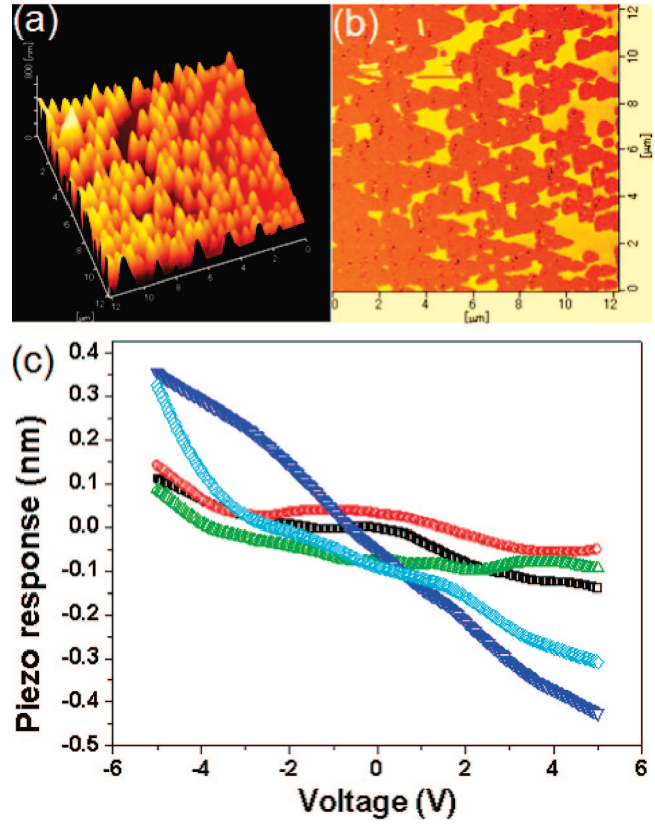


**Figure 4.** (a) AFM and (b) PRM images of ZnO nanorods grown on the PPI ZnO template. (c) Voltage-piezo response of separated single ZnO nanorods on the template.

Following the deposition of Au films with a thickness of 10 Å on the surface of a PPI template, we used chemical vapor transport and condensation for the growth of ZnO nanorods at 900 °C for 20 min under a mixed gas flow of Ar and $O_2$ (5%) controlled at 100 sccm.

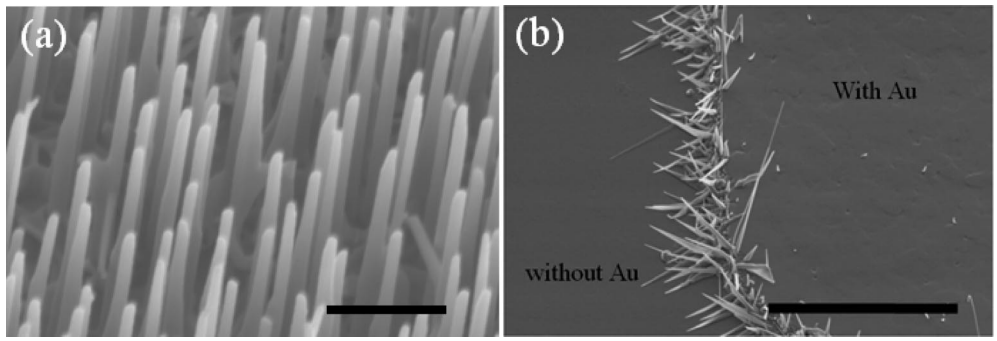


**Figure 5.** Tilting view SEM image of the surface morphology after the growth of ZnO on the (a) Zn- and (b) O-polar ZnO template. The scale bar is 1 $\mu$m.

Figure 3a,b shows spatially separated vertical ZnO nanorod arrays with a pitch of ~650 nm on the PPI ZnO template. The SEM image in Figure 3b reveals that ZnO nanorods are formed only on Zn-polar regions. The diameter and length of nanorods measure about 145 ± 27 nm and 6.37 ± 0.4 $\mu$m, respectively, which indicates superior control of both diameter and length of nanorods. The spatial separation between nanorods was also confirmed by observation of optical microscopy as shown in Figure 3c due to waveguide effects about visible emission in ZnO nanorods. Figure 3d,e shows the distribution of distance between neighbor nanorods along the PPI structure (*x*-axis) and perpendicular to the PPI structure (*y*-axis). The average separation of adjacent rods along *x*- and *y*-axis is 1.1 ± 0.34 $\mu$m and 0.65 ± 0.06 $\mu$m, respectively. The mean rod−rod distance perpendicular to the PPI structure is limited by the separation between the adjacent Zn-polar ZnO stripes, which is ~650 nm. Hence excellent controllability of the growth site has been achieved. On the other, the mean separation of adjacent nanorods on the same Zn-polar ZnO stripes is also observed. The following two possible reasons could be considered as factors affecting the separation of nanorods on *y*-axis. One is the Au particles distribution in a catalytic growth, and the other is the migration length of adatoms on Zn-polar surface at high growth temperature. The position of Au droplet on substrate surface is basically limited by dewetting of Au layer and surface migration length of Au atoms with increasing temperature.[14] In order to compare with the distribution of the nanorods on the PPI template, we performed annealing of each polar surface with predeposited Au film at the growth temperature (Supporting Information, Figure S1 and Table S1). It is confirmed that the distribution of Au particles is almost independent with the polarity and with the spatial separation of nanorods. The migration length of adatoms as the other factor is decided on the diffusion coefficient and the lifetime of adatoms at the surface.[15] We employed a PPI template with pitch of 5 $\mu$m to avoid the limitation by the effect of pitch size in the PPI structure. The distance of between center-to-center of neighbor nanostructures is found to be about 0.82 ± 0.3 $\mu$m, which is similar with the result of ZnO nanorods on the *y*-axis in Figure 3. (Supporting Information, Figure 2S) It could be concluded that the nucleation on the surface of Zn-polar ZnO forms with the gap due to migration length of adatoms and finally leads to a separation of nanorods.

The polarity of ZnO nanorods was confirmed using a piezo-response of AFM tip due to surface charge of ZnO after confirming the site of ZnO nanorods on the PPI template through AFM and PRM measurement as shown in Figure 4a,b. The AC input voltage in the range from −5 to 5 V was applied to an AFM tip on the top surface of single ZnO nanorod, which resulted in decreasing the piezo-response when increasing the voltage as shown in Figure 4c. These features are due to a negative field with respect to the [0001] direction and the contraction of Zn-polar ZnO nanorods. The difference of piezo-response range for several nanorods is probable due to the nanorod diameter, length, and tip contact positions.

A possible growth mechanism of the ZnO nanorods on the polar ZnO structures is discussed in the following. At first, we can expect the higher reactivity such as the formation Au−Zn alloy or diffusion of Zn into Au particles on Zn-polar surface at growth temperature.[16,17] In the case of O-polar surface, the surface is terminated by oxygen atoms, in which each oxygen atom at the surface is bonded to three Zn atoms located in the layer just below the surface oxygen layer. Such a situation will prevent the reaction between Au and Zn. Second, the surface properties of the substrate strongly affect the growth behaviors of the ZnO nanostructure. As mentioned above, Zn-polar ZnO has a higher growth rate than O-polar ZnO due to the dangling bond configuration at the surface. Under oxygen atmosphere, each O atom on a Zn-polar ZnO surface has three dangling bonds, while each O atom at the O-polar ZnO surface has a single dangling bond along the *c*-axis. Such different configuration of dangling bonds affects the incorporation rate of Zn atoms on each surface. In addition, the Zn-polar growth will be enhanced because of higher surface energy of Zn-polar ZnO surface than O-polar surface.

Through experiments using MBE grown ZnO thin film with single polarity, it was confirmed that ZnO laterally grew on Au-predeposited O-polar ZnO layers, while the growth of nanorods dominated on Zn-polar ZnO surface. We prepared Zn-polar and O-polar ZnO templates separately by MBE, in which the thickness of the MgO buffer layer was changed.[12] One nanometer thick Au films were deposited both on the O-polar and Zn-polar ZnO templates by electron-beam evaporation and were patterned by photolithography. After growth of ZnO nanorods under the previously described growth conditions, the surface morphology was observed by

SEM as shown in Figure 5. It was found that ZnO nanorods formed vertically on the Zn-polar template (Figure 5a). On the other hand on the O-polar ZnO template, ZnO were two-dimensionally grown on the region of O-polar ZnO with Au and some nanostructurs were formed at side facet of the boundary of Au deposited region as shown in Figure 5b. Such difference in growth morphology can be understood in terms of the difference of surface energy between the two polar surfaces.

In summary, we have achieved the growth of highly ordered ZnO nanorod arrays with submicron gaps by exploiting the nature of polar ZnO surfaces. The fabricated ZnO nanorod arrays are Zn-polar and the position, density, and diameter of ZnO nanorods are well controlled by the polarity of template. These features provide the effect of the polarity on the growth of ZnO nanostructures and can also be useful for nanoelectronics and optoelectronic devices.

**Acknowledgment.** A part of this work is supported by the Research Fellowships for Young Scientists Program of the Japan Society for the Promotion of Science (JSPS).

**Supporting Information Available:** Figure S1 shows the surface morphology of each sample after annealing. Figure S2 shows the growth result of ZnO on a PPI template with 5 $\mu$m pitch at 900 °C for 20 min. Table S1 lists the diameter, particle density, and the approximate gap with adjacent particles of Au particles on O- and Zn-polar ZnO after annealing at 900 °C. This material is available free of charge via the Internet at http://pubs.acs.org.

## References

(1) Tans, S. J.; Verschuerene, A. R. M.; Dekker, C. *Nature* **1998**, *393*, 49.
(2) Cui, Y.; Wei, Q.; Park, H.; Lieber, C. M. *Science* **2001**, *293*, 1289.
(3) Yan, H.; He, R.; Johnson, J.; Law, M.; Saykally, R. J.; Yang, P. *J. Am. Chem. Soc.* **2003**, *125*, 4728.
(4) Fan, H. J.; Werner, P.; Zacharias, M. *Small* **2006**, *2*, 702.
(5) Kar, S.; Pal, B. N.; Chaudhuri, S.; Chakravorty, D. *J. Phys. Chem. B* **2006**, *110*, 4605.
(6) Huang, H. M.; Mao, S.; Feick, H.; Yan, H. Q.; Wu, Y. Y.; Kind, H.; Weber, E.; Russo, R.; Yang, P. D. *Science* **2001**, *292*, 1897.
(7) Wang, Z. L.; Song, J. *Science* **2006**, *312*, 242.
(8) Wang, Z. L.; Kong, X. Y.; Zuo, J. M. *Phys. Rev. Lett.* **2003**, *91*, 185502.
(9) Gao, P. X.; Wang, Z. L. *J. Phys. Chem. B* **2004**, *108*, 7534.
(10) Kato, H.; Miyamoto, K.; Sano, M.; Yao, T. *Appl. Phys. Lett.* **2004**, *84*, 4562.
(11) Park, J.; Hong, S. K.; Minegishi, T.; Park, S. H.; Im, I. H.; Hanada, T.; Cho, M. H.; Yao, T.; Lee, J. W.; Lee, Y. L. *Appl. Phys. Lett.* **2007**, *90*, 201907.
(12) Minegishi, T.; Yoo, J. H.; Suzuki, H.; Vashaei, Z.; Inaba, K.; Shim, K. S.; Yao, T. *J. Vac. Soc. Technol., B* **2005**, *23*, 1286.
(13) Cho, C. -O.; Jeong, J.; Lee, J.; Jeon, H.; Kim, I.; Jang, D. H.; Park, Y. S.; Woo, J. C. *Appl. Phys. Lett.* **2005**, *87*, 161102.
(14) Hannon, J. B.; Kodambaka, S.; Ross, F. M.; Tromp, R. M. *Nature* **2006**, *440*, 69.
(15) Sano, M.; Miyamoto, K.; Kato, H.; Yao, T. *J. Appl. Phys.* **2004**, *95*, 5527.
(16) Okamoto, H.; Massalski, T. B. In *Binary Alloy Phase Diagrams*; Massalski, T. B., Murry, J. L., Bennett, L. H., Baker, H., Kacprzak, L., Eds.; American Society for Metals: Metals Park, OH, 1986.
(17) Kirkham, M.; Wang, X.; Wang, Z. L.; Snyder, R. L. *Nanotechnology* **2007**, *18*, 365304.

NL801344S